Article:

Enara Fernandez, Maider Amutio, Maite Artetxe, Aitor Arregi, Laura Santamaria, Gartzen Lopez, Javier Bilbao, Martin Olazar. ***Assessment of product yields and catalyst deactivation in fixed and fluidized bed reactors in the steam reforming of biomass pyrolysis volatiles***. **Process Safety and Environmental Protection** 145 : 52–62 (2021)

Received 19 June 2020, Revised 24 July 2020, Accepted 25 July 2020, Available online 2 August 2020.

https://doi.org/10.1016/j.psep.2020.07.039

Assessment of product yields and catalyst deactivation in fixed and fluidized bed reactors in the steam reforming of biomass pyrolysis volatiles

Enara Fernandez[a], Maider Amutio[a], Maite Artetxe[a], Aitor Arregi[a], Laura Santamaria[a], Gartzen Lopez[a,b], Javier Bilbao[a], Martin Olazar[a]

[a]Department of Chemical Engineering, University of the Basque Country UPV/EHU, P.O. Box 644 - E48080 Bilbao (Spain).

[b]IKERBASQUE, Basque Foundation for Science, Bilbao, Spain

Abstract

The performance of fixed and fluidized bed reactors in the steam reforming of biomass fast pyrolysis volatiles was compared, with especial attention paying to the differences observed in catalysts deactivation. The experiments were carried out in continuous regime in a bench scale unit provided with a conical spouted bed for the pyrolysis step. They were carried out on a Ni-Ca/Al_2O_3 commercial catalyst and under optimum conditions determined in previous studies, i.e., pyrolysis temperature 500 ºC, reforming temperature 600 ºC and a steam/biomass ratio of 4. Moreover, the influence of space time was analysed in both reforming reactors. The fixed bed reactor showed higher initial conversion and H_2 yield, as it allowed attaining a H_2 yield higher than 90 % with a space time of 10 g_{cat} min g_{vol}^{-1}. However, a space time of 15 g_{cat} min g_{vol}^{-1} was required in the fluidized bed to obtain a similar H_2 yield. Moreover, the fixed bed also led to lower catalyst deactivation. Catalyst deactivation was mainly related to coke deposition, and higher coke contents were observed in the catalysts used in the fluidized bed reactor (1.2 mg_{COKE} g_{cat}^{-1} $g_{biomass}^{-1}$) than those in the fixed bed one (0.6 mg_{COKE} g_{cat}^{-1}

$g_{biomass}^{-1}$). Therefore, the differences in the performance of the two reactors were analysed and their practical interest was discussed.

Keywords: hydrogen; pyrolysis; reforming; biomass; deactivation; fixed bed; fluidized bed

1. Introduction

The environmental concerns associated with global warming are promoting the development of alternative processes for the production of fuels and chemicals. Within this scenario, biomass may play a relevant role in the implementation of sustainable routes contributing to the reduction of CO_2 emissions. The production of hydrogen from biomass is of especial interest, as it is a material with high specific energy density and highly versatile as fuel and raw material (Shahabuddin et al., 2020). It is to note that the current hydrogen production is mainly based on the gasification and steam reforming of non-renewable sources, such as coal, natural gas and oil (Parthasarathy and Narayanan, 2014; Arregi et al., 2018a).

A wide variety of thermochemical conversion processes have been proposed for hydrogen production from biomass (Balat and Kirtay, 2010; Tanksale, Beltramini and Lu, 2010; Shahabuddin et al., 2020; Arregi et al., 2018a; Pandey, Prajapati and Sheth, 2019). Amongst them, the direct route of biomass steam gasification is an alternative with a considerable technological development (Molino, Chianese and Musmarra, 2016; Heidenreich and Foscolo, 2015; Claude et al., 2016). However, this process faces challenges that hinder its implementation, especially the excessive tar content in the syngas (Valderrama Rios et al., 2018; Shen and Yoshikawa, 2013; Font Palma, 2013; Kaewpanha et al., 2017; Adnan et al., 2018). The steam reforming of biomass fast pyrolysis oil (bio-oil) has been extensively studied as an indirect delocalized alternative

(Chen, Sun and Wang, 2017a; Nabgan et al., 2017). The main challenges of this process are associated with the complex nature of the bio-oil and its handling, especially during storage, feeding and vaporization (Trane et al., 2012; Basagiannis and Verykios, 2007; Arregi et al., 2018a).

More recently, the process of biomass pyrolysis-reforming was proposed in order to overcome the problems associated with bio-oil reforming. In this strategy, the steps of biomass pyrolysis and the in-line steam reforming of the volatiles leaving the first reactor are integrated in a single process. The main advantages of this strategy are as follows: i) contact of reforming catalysts with biomass impurities is avoided, as they remain in the pyrolysis reactor, ii) independent temperature optimization in the pyrolysis and reforming steps can be performed, iii) process temperature is reduced with respect to conventional steam gasification, iv) a gas product with high hydrogen content and free of tars can be obtained (Lopez et al., 2018; Arregi et al., 2018a). Thus, hydrogen yields in the 4 to 10 wt% range have been reported in the biomass pyrolysis-reforming conducted under suitable conditions (Yu et al., 2019; Gai et al., 2019; Santamaria et al., 2018; Santamaria et al., 2020; Miyazawa et al., 2006; Xiao et al., 2011; Cao et al., 2014; Bunma and Kuchonthara, 2018). The high versatility of this strategy has been proven, as it may treat other solid wastes, such as plastics or mixtures of plastics and biomass (Chai et al., 2020; Arregi et al., 2017; Alvarez et al., 2014; Kumagai et al., 2015). Interestingly, the higher hydrogen content of plastics led to higher hydrogen productions (Barbarias et al., 2016; Barbarias et al., 2018b; Park et al., 2010; Wu and Williams, 2010).

In spite of the potential interest of the pyrolysis-reforming strategy, the technical development of the process is limited and most of the studies in the literature are of preliminary nature, as they have been mainly performed in lab scale units under batch

conditions (Lopez et al., 2018; Arregi et al., 2018a). In fact, the most studied reactor configuration is made up of two fixed bed reactors operating in batch regime (Chen et al., 2016; Dong et al., 2017; Cao et al., 2014; Shen et al., 2014; Kumagai et al., 2019). Prof. Tomishige et al. also proposed a process based on two lab scale fixed bed reactors for biomass pyrolysis reforming, and they operated with continuous biomass feed (Wang et al., 2011; Wang et al., 2013). Xiao et al. (Xiao et al., 2013; Xiao et al., 2011) developed a continuous bench reaction system that combined a fluidized bed reactor for biomass pyrolysis and a fixed bed for the catalytic steam reforming. In the continuous process implemented by Efika et al. (Efika, Wu and Williams, 2012), a screw kiln coupled with a fixed bed was used. The research group headed by Prof. Olazar proposed a bench scale continuous unit by combining a conical spouted bed for biomass fast pyrolysis and a fluidized bed reactor for the subsequent reforming of pyrolysis volatiles (Arregi et al., 2016; Santamaria et al., 2019a; Arregi et al., 2018b; Santamaria et al., 2018).

In order to progress in the technical development of the pyrolysis and in-line reforming strategy, and understand the role played by the reforming reactor, catalyst deactivation is compared in this study by using a fixed bed and a fluidized bed reactor in the reforming step. The pyrolysis reactor is a conical spouted bed in both cases, as it performs well in biomass and waste processing (Moliner et al., 2017; Perkins, Bhaskar and Konarova, 2018; Lopez et al., 2017). It is to note that the spouted bed-fixed bed configuration was tested for the first time in the pyrolysis reforming of waste plastics (Erkiaga et al., 2015). However, operation with this feed and a fixed bed regime in the reforming step led to excessive coke formation and subsequent operational problems associated with bed plugging. These problems, which were only observed in waste plastic valorization, are avoided in the fluidized bed reactor due to the vigorous

movement of the particles in this reactor. The aim of this research is to analyze the influence the reforming reactor configuration has on the performance of the overall process of biomass pyrolysis-reforming, considering not only the conversion of pyrolysis volatiles and hydrogen production, but also catalyst deactivation and the evaluation of its causes. Moreover, the relationship between the concentration of oxygenated compounds (main coke precursors) and coke deposition was analyzed in both reactors. These results obtained operating in continuous regime provide relevant information for the full scale reactor design.

2. Experimental

2.1. Materials

The biomass selected to perform this study was pine wood (pinus insignis), which is highly abundant in Europe and representative of softwoods. The particle size used in the experiments was in the 1 to 2 mm range in order to ensure a suitable operation of the solid feeding system. The characterization of this biomass includes ultimate analysis (LECO CHNS-932 elemental analyzer), proximate analysis (TGA Q500IR thermogravimetric analyzer) and the determination of the higher heating value (HHV) (Parr 1356 isoperibolic bomb calorimeter). The results obtained are summarized in Table 1.

Table 1. Pine wood sawdust characterization.

Ultimate analysis (wt%)[a]	
Carbon	49.33
Hydrogen	6.06
Nitrogen	0.04
Oxygen[b]	44.57
Proximate analysis (wt%)[c]	
Volatile matter	73.4
Fixed carbon	16.7
Ash	0.5
Moisture	9.4

HHV (MJ kg^{-1})	19.8

[a] on a dry basis
[b] by difference
[c] on an air-dried basis

In order to ease the comparison of the results obtained in the reforming steps performed in fixed and fluidized bed reactors, a commercial reforming catalyst supplied by Süd Chemie (G90LDP catalyst) was used. The active metallic phase is Ni, which is supported on Al_2O_3 and doped with Ca. The NiO content in the catalyst is 14 wt.%. The original catalyst was ground and sieved to obtain a particle size between 0.4 and 0.8 mm, which was determined as the optimum one to ensure a stable fluidization regime (Arregi et al., 2016). In order to avoid kinetic effects associated with internal mass transfer limitations, the same catalyst particle size was used in the fixed bed reactor.

The porous structure of this catalyst was analyzed by N_2 adsorption-desorption in a Micromeritics ASAP 2010. The BET surface area is 19 m^2 g^{-1} and the average pore diameter 122 Å. The adsorption-desorption isotherm of the catalyst and further details of this analysis are described elsewhere (Erkiaga et al., 2015). The reducibility of the catalyst was evaluated in an AutoChem II 2920 Micromeritics. The TPR curve was reported elsewhere (Erkiaga et al., 2015) and shows two reduction steps, the main peak at 550 ºC associated with the reduction of NiO interacting with α-Al_2O_3, and another peak at 700 ºC, which is related to $NiAl_2O_4$ reduction. According to the results obtained in the TPR analysis, the conditions established for the in situ reduction prior to use are a temperature of 710 ºC for 4 h under 10% vol. H_2 stream.

The coke in the deactivated catalysts was analyzed by Temperature Programmed Oxidation (TPO) in a Thermobalance (SDT 2960 T.A. Instruments) coupled to a mass spectrometer (Thermostar Balzers Instrument). The procedure includes stabilization of the signal with a N_2 stream (10 mL min^{-1}) at 100 ºC, and a subsequent step of oxidation under air (50 mL min^{-1}) atmosphere with a heating ramp of 5 ºC min^{-1} to 800 ºC, with this temperature being kept for 30 min to ensure full combustion of the coke.

2.2. Reaction equipment

The experiments were carried out in a bench scale unit that operates in continuous regime, whose scheme is shown in Figure 1. The pyrolysis reaction was performed in a conical spouted bed reactor (CSBR). This reactor's design ensures high heat and mass transfer rates, high turbulence (close to perfect mix) for the solid phase and short residence times for the pyrolysis volatiles. The excellent performance of the CSBR was demonstrated in the fast pyrolysis of different solid wastes, such as biomass (Alvarez et al., 2018; Amutio et al., 2012), plastics (Artetxe et al., 2015; Barbarias et al., 2016) and tires (Alvarez et al., 2019; Alvarez et al., 2017).

The dimensions of the CSBR are based on previous hydrodynamic studies and guarantee a stable operation in a wide range of gas flow rates. The detailed reactor design can be found elsewhere (Barbarias et al., 2016; Arregi et al., 2016).

The reforming of the pyrolysis volatiles was performed in-line in a second reactor by operating in either fixed or fluidized bed regime depending on the location of the gas inlet. Thus, the gas was introduced through the bottom of the reactor (upward flow) to attain a fluidization regime, whereas it was introduced through the top (downward flow) to operate in fixed bed. The main dimensions of this reactor are described elsewhere (Barbarias et al., 2016; Arregi et al., 2016).

The gas cleaning system includes a cyclone located between pyrolysis and reforming reactors to retain fine particles, mainly char. Moreover, in the experiments performed in the fluidized bed regime, a sintered steel filter was placed downstream to recover the elutriated catalyst fines. Both reactors (pyrolyser and reformer) and the gas cleaning elements were located in a forced convection oven maintained at high temperature to prevent the condensation of steam and pyrolysis volatile compounds.

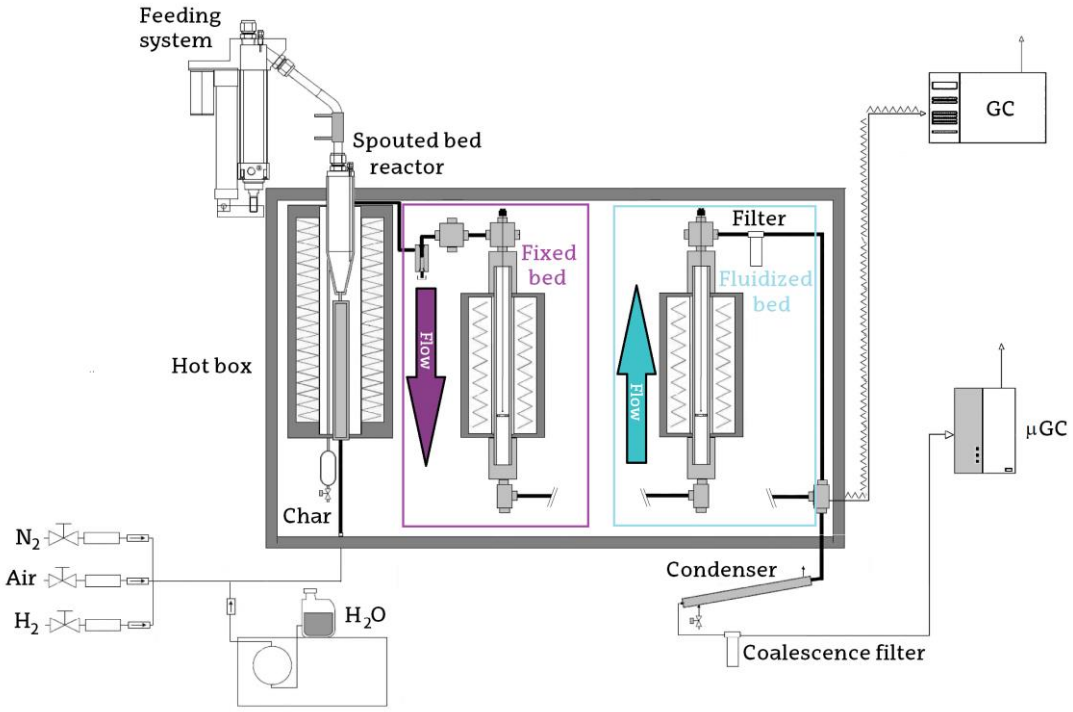

Figure 1. Diagrammatic representation of the bench scale plant for continuous pyrolysis-reforming of biomass with fixed and fluidized bed configurations in the reforming step.

The reaction unit is equipped with devices for continuously feeding biomass, water and gases (N_2, air, H_2), analyzing the volatile stream and incondensable gases and condensing the outlet stream (Figure 1). The biomass feeding system enables operating in continuous regime and is made up of a cylindrical vessel equipped with a vertical shaft connected to a piston placed below the biomass bed. A vibration system is actuated at the same time as the piston rises, and so the feed is discharged into the

reactor through a pipe cooled with tap water. Moreover, in order to avoid the entrance of the volatile stream into the feeding vessel, a small N_2 flow rate is introduced into the feeder.

A high precision Gilson 307 pump was used to measure the water flow rate. Water is vaporized prior to entering the forced convection oven by means of a heating cartridge located inside the hot box, and is then fed into the pyrolysis reactor. The utilization of steam as fluidizing agent in the pyrolysis reactor instead of an inert gas (as N_2) avoids the dilution of the gaseous stream in the reforming reactor and eases the condensation of the volatile products (non-reacted oxygenates and water). Previous studies have proven that use of steam instead of N_2 in the pyrolysis step at 500ºC has little influence on product distribution (Arregi et al., 2016). In addition, N_2, air and H_2 can be fed into the pyrolysis reactor, i.e., N_2 is used as fluidizing agent during the heating process and H_2 to reduce the Ni catalyst prior to the reforming reaction.

The analysis of the volatiles leaving both the pyrolysis reactor and the reforming reactor was carried out on-line by means of a GC Agilent 6890, provided with a HP-Pona column (50 m length, 0.2 mm diameter and 0.5 μm film thickness) and a flame ionization detector (FID). The sample was injected into the GC by means of a line thermostated at 280 ºC, once the reforming reactor outlet stream was diluted with an inert gas. A micro GC (Varian 4900) was used to analyze on-line the non-condensable gases once the outlet stream of the reforming reactor was condensed (cooled with tap water) and filtered (coalescence element). Both the GC and the microGC analyses were carried out subsequent to several minute operation to ensure steady state conditions. It is to note that the micro GC and conventional GC analyses were carried out every 3 and 20 minutes, respectively, due to the different duration of the analyses. Furthermore, the reproducibility of the results was guaranteed by repeating the analyses at least 3 times

under the same conditions. The determination of product flow rates, yields and the amount of reacted steam was assessed based on the overall and elemental (C, H and O) mass balance closure considering the composition of the products entering the reforming step (pyrolysis volatile stream) and the information gathered in the GC and microGC analyses. It is to note that the carbon deposited on the catalyst was not considered in the mass balance closure, as it means less than 0.5 % of all the carbon contained in the treated biomass.

2.3. Experimental conditions

The determination of suitable operating conditions in the two-step pyrolysis-reforming process is crucial, as steam is the spouting agent in the pyrolysis step, but also the fluidizing agent (fluidized bed reformer) or carrier gas (fixed bed reformer) in the reforming step. In order to attain an appropriate spouting regime, a bed of 50 g of silica sand with a particle size in the 0.3-0.35 mm range was used in the CSBR. The selection of the particle sizes of catalyst and sand in the reforming step was conditioned by the hydrodynamic performance of the fluidized bed. It is to note that the same particle size as in the fluidized bed was used in the fixed bed, with this point being of special relevance in the case of the catalyst, as its modification may affect mass transfer within the catalyst, and therefore reforming activity. Based on the performance observed in previous studies (Barbarias et al., 2016; Arregi et al., 2016), the bed was made up of a mixture of reforming catalyst and inert sand, with the total mass being 25 g. The ratio between catalyst and sand was varied depending on the space time used in the reforming process. The particle size of the catalyst was in the 0.4-0.8 mm range and that of the inert silica sand in the 0.3-0.35 mm range when operation was carried out in fluidized bed regime. Thus, both materials have similar minimum fluidization velocities, and operation in the fluidized bed was conducted with a velocity of approximately two times

the minimum one. In the fixed bed, the size of sand particles was bigger (1-2 mm range) in order to reduce bed pressure drop and that of catalyst particles the same as in the fluidized bed. It should be pointed out that the interest of using different particle sizes of the sand and catalysts lies in their separation by sieving at the end of the experiment.

A temperature of 500 ºC was selected for the pyrolysis step, as it is the optimum one to maximize bio-oil yield in the pyrolysis of different biomasses (Amutio et al., 2012; Alvarez et al., 2018). These high bio-oil yields are due to the short residence times (below 0.5 s) and high heating rates (10^3-10^4 ºC min^{-1}) attained in the spouted bed reactor. In the case of the catalytic steam reforming, the process was conducted at 600 ºC, as a further increase to 700 ºC hardly improved the experimental results (Arregi et al., 2016) and led to Ni sintering (Moulijn, Van Diepen and Kapteijn, 2010). The steam/biomass (S/B) ratio was fixed in all the experiments in a value of 4, with pine wood feed rate being 0.75 g min^{-1} and that of water 3 ml min^{-1}. This S/B ratio corresponds to a molar steam/carbon (S/C) ratio of 7.7. In order to compare the performance of fixed and fluidized bed reactors, the reforming of biomass pyrolysis volatiles was conducted using different space times, i.e., 2.5, 5, 10 and 20 g_{cat} min $g_{volatiles}^{-1}$.

2.4. Reaction indexes

The reforming step conversion, individual product yields and hydrogen production were considered as the main reaction indexes for the assessment of fixed and fluidized bed performance. Reforming conversion was defined as the ratio between the C equivalent units in the gaseous product and those in the feed of the reforming step:

$$X = \frac{C_{gas}}{C_{volatiles}} 100 \quad (1)$$

It should be noted that the C amount contained in the char produced in the pyrolysis step was not considered in Eq (1).

The yield of each individual product was calculated as:

$$Y_i = \frac{F_i}{F_{volatiles}} 100 \quad (2)$$

where F_i and $F_{volatiles}$ are the molar flow rates of product i and the pyrolysis volatiles at the inlet of the reforming reactor, respectively, both given in C equivalent units (C moles/time unit).

The hydrogen yield was defined based on the maximum allowable by stoichiometry:

$$Y_{H_2} = \frac{F_{H_2}}{F^0_{H_2}} 100 \quad (3)$$

where F_{H2} is the H_2 molar flow rate and F^0_{H2} the maximum allowable by the following stoichiometry corresponding to the composition of pyrolysis volatiles ($C_nH_mO_k$):

$$C_nH_mO_k + (2n-k)H_2O \rightarrow nCO_2 + (2n+m/2-k)H_2 \quad (4)$$

H_2 production was calculated as the mass of H_2 produced per biomass mass unit fed into the pyrolysis step:

$$P_{H_2} = \frac{m_{H_2}}{m^0_{Biomass}} 100 \quad (5)$$

3. Results

3.1. Analysis of pyrolysis products

Prior to evaluating the influence the type of reforming reactor has on process performance, the product stream obtained in the pyrolysis step was characterized. Table 1 shows the product distribution obtained in the biomass pyrolysis performed at 500 ºC in the conical spouted bed reactor. The fast pyrolysis conditions attained in this reactor, i.e., short residence time and high heating rates, led to a high bio-oil yield (75.3 wt.%), which is evidence of the suitable features of this reactor for solid waste valorisation by pyrolysis (Garcia-Nunez et al., 2017; Lopez et al., 2017; Perkins, Bhaskar and

Konarova, 2018). As observed in Table 1, the bio-oil has a complex composition including different families of oxygenated compounds (acids, aldehydes, alcohols, ketones, phenols, furans and saccharides), as well as a high water content stemmed from dehydration reactions and biomass moisture.

The gas yield obtained is low, 7.5 wt.%, and made up of mainly CO and CO_2 with minor contents of methane, light hydrocarbons and hydrogen. The char yield was of 17.3 wt.% and was continuously removed from the bed through a lateral outlet to avoid its accumulation. The mentioned product distribution led to the following carbon distribution amongst pyrolysis products: 7.1 % in the gas, 63.8 % in the bio-oil and 29.1 %in the char.

Table 1. Product distribution obtained in the pyrolysis step at 500 ºC.

Compound	Yield (wt %)
Gas	**7.3 ± 0.34**
CO	3.38 ± 0.16
CO_2	3.27 ± 0.15
CH_4	0.36 ± 0.02
Hydrocarbons (C_2-C_4)	0.3 ± 0.01
H_2	0.04 ± 0.002
Bio-oil	**75.3** ± 3.5
Acids	2.73 ± 0.13
Aldehydes	1.93 ± 0.09
Alcohols	2 ± 0.09
Ketones	6.37 ± 0.30
Phenols	16.49 ± 0.78
Furans	3.32 ± 0.15
Saccharides	4.46 ± 0.21
Water	25.36 ± 1.20
Char	**17.3 ± 0.72**

3.2. Products yields at zero time on stream

In order to compare the performance of the reforming process in fixed and fluidised bed regimes, the conversion of pyrolysis volatiles was compared by operating with different space times (Figure 2). The runs were performed under the same conditions, i.e., pyrolysis and reforming temperatures of 500 and 600 ºC, respectively, and a S/B ratio of 4. The following main reactions are considered in the reforming process:

Oxygenate steam reforming: $Oxygenates + H_2O \rightarrow CO + H_2$ (6)

Water gas shift (WGS) reaction: $CO + H_2O \Leftrightarrow CO_2 + H_2$ (7)

Oxygenate cracking (secondary reaction):

$C_nH_mO_k \rightarrow oxygenates + hydrocarbons + CH_4 + CO + CO_2$ (8)

Methane (and hydrocarbons) steam reforming: $CH_4 + H_2O \Leftrightarrow CO + 3H_2$ (9)

Remarkable differences are observed in Figure 2 between the conversions obtained in fixed and fluidized bed reactors. The fixed bed reactor led to higher conversion values for all the space times studied, with this effect being more significant operating with low space time values. Thus, a space time of 10 g_{cat} min g_{vol}^{-1} was enough for the fixed bed reactor to attain almost full conversion (>98%). However, when the reactor operated in fluidized bed regime, a space time of 15 g_{cat} min g_{vol}^{-1} was required to obtain a similar conversion. Furthermore, great differences were observed when low space times were used. Thus, a space time of 2.5 g_{cat} min g_{vol}^{-1} in the fixed bed reactor led to a conversion of 75.9 %, whereas that obtained in the fluidized bed reactor was of 27.3 %. These results clearly evidence the higher efficiency in the transformation of pyrolysis volatiles when the catalyst is used under fixed bed reactor conditions. This different performance should be attributed to the different contact between the catalyst and gaseous stream in the two configurations used. Thus, the gas flow pattern in fluidized beds is much more complex than in fixed ones, as a fraction of the gas crosses the bed through the dense phase, whereas the remaining fraction does it in the form of bubbles

(Kunii and Levenspiel, 2013). Thus, the dense phase has a relatively low porosity, with almost the whole bed solid inventory being in this phase, whereas the bubble phase has a porosity close to 1, as very few particles are within the bubbles. Accordingly, the contact in the dense phase is efficient, and conversion rate in this phase is therefore high. However, there is almost no contact between the catalyst and gaseous products in the bubbles and, furthermore, there are also diffusional restrictions for reactant transfer from the bubbles to the dense phase. Therefore, the flow regime in the bubbling fluidized bed leads to a fraction of gas bypassing the contact with the catalyst, and the subsequent reduction in conversion. In addition, the gas flow rate in the reforming reactor decreased slightly with the advance of catalyst deactivation, which involves an additional challenge to attain plug flow contact. The poorer contact with the catalyst attained in fluidized beds with respect to that in fixed beds explains the lower conversion attained in the former using the same space time (Figure 2). Similar conclusions were reported by Remon et al. (Remón et al., 2014; Remon et al., 2013) when they compared the performance of fixed and fluidized bed reactors in bio-oil reforming. However, Lan et al. (Lan et al., 2010) reported higher hydrogen yields in a fluidized bed reactor than in a fixed bed. Nevertheless, their experiments in the fluidized bed were carried out with higher S/C ratios, with this fact hindering a suitable comparison because an increase in this parameter promotes reforming and WGS reactions, and therefore enhances hydrogen production (Arregi et al., 2016; Liu et al., 2013; Fu et al., 2014a; Gao et al., 2015).

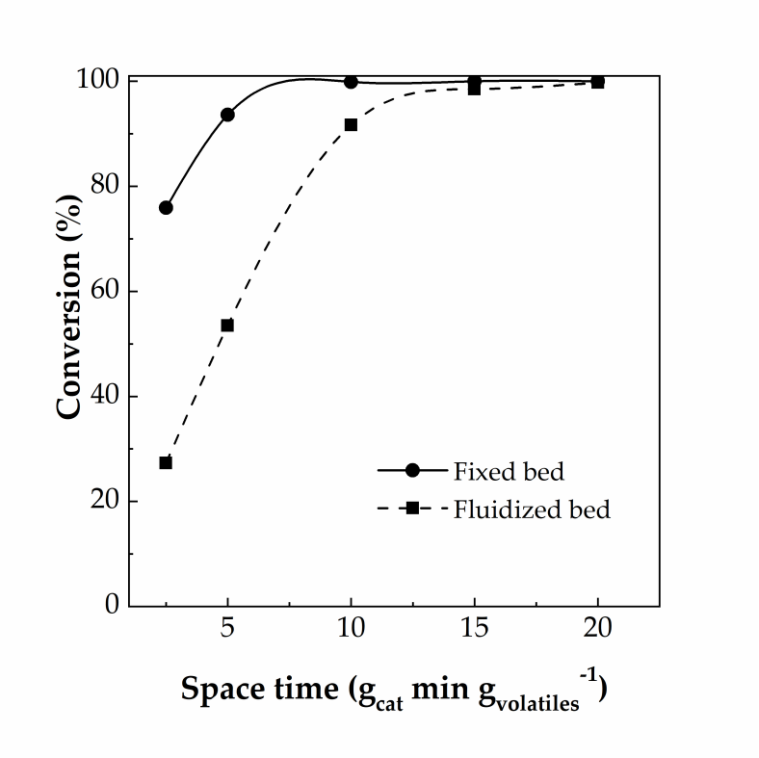

Figure 2. Comparison of the reforming step conversion at zero time on stream in fixed and fluidized bed reactors for several space times.

Figure 3 shows the evolution of individual product yields with space time obtained operating under fixed and fluidized bed conditions. These results also evidence the higher efficiency of the fixed bed for the catalytic conversion of biomass derived volatiles. In fact, higher H_2 and CO_2 yields were obtained in the fixed bed than in the fluidized bed reactor operating with the same space time. Regardless of the reactor used, an increase in space time to 20 g_{cat} min g_{vol}^{-1} ensured full conversion of biomass derived oxygenates to gaseous product due to the displacement of reforming reactions. Under these conditions, H_2 and CO_2 yields were only slightly lower in the fluidized bed with respect to those obtained in the fixed bed, 93.4, 88.5 vs. 94.2, 89.3 %, respectively. It is to note that these high hydrogen yields correspond to production values of around 11 wt% in both reforming reactor designs.

These results clearly reveal the potential of the two-step process consisting of a spouted bed reactor for biomass fast pyrolysis and a fluidized or fixed bed reactor for the in-line

reforming of pyrolysis volatiles. It should be noted that the results reported in the literature are generally lower than those obtained in this study with a space time of 20 g_{cat} min g_{vol}^{-1}. Thus, Xiao et al. reported a hydrogen production of 10 wt.% using Ni supported on coal char in a reaction unit made up of two fixed bed reactors (Xiao et al., 2013). Operating in a similar experimental unit with a Ni/Al_2O_3 catalyst, Cao et al. (Cao et al., 2014) obtained a hydrogen production of 11.6 wt.% in the reforming of sewage sludge pyrolysis volatiles. However, it should be noted that this yield was reported on a dry ash-free basis. The same authors also studied the reforming of biomass pyrolysis volatiles in a continuous unit with a fluidized bed for the pyrolysis step and a fixed bed for the reforming one, reporting a maximum hydrogen yield of 9.3 wt.% (Xiao et al., 2011). Recently, Gai et al. (Gai et al., 2019) obtained a high hydrogen yield (10.9 wt.%) in the reforming of sewage sludge volatiles on Ni/hydrochar in a batch reaction system including two fixed bed reactors.

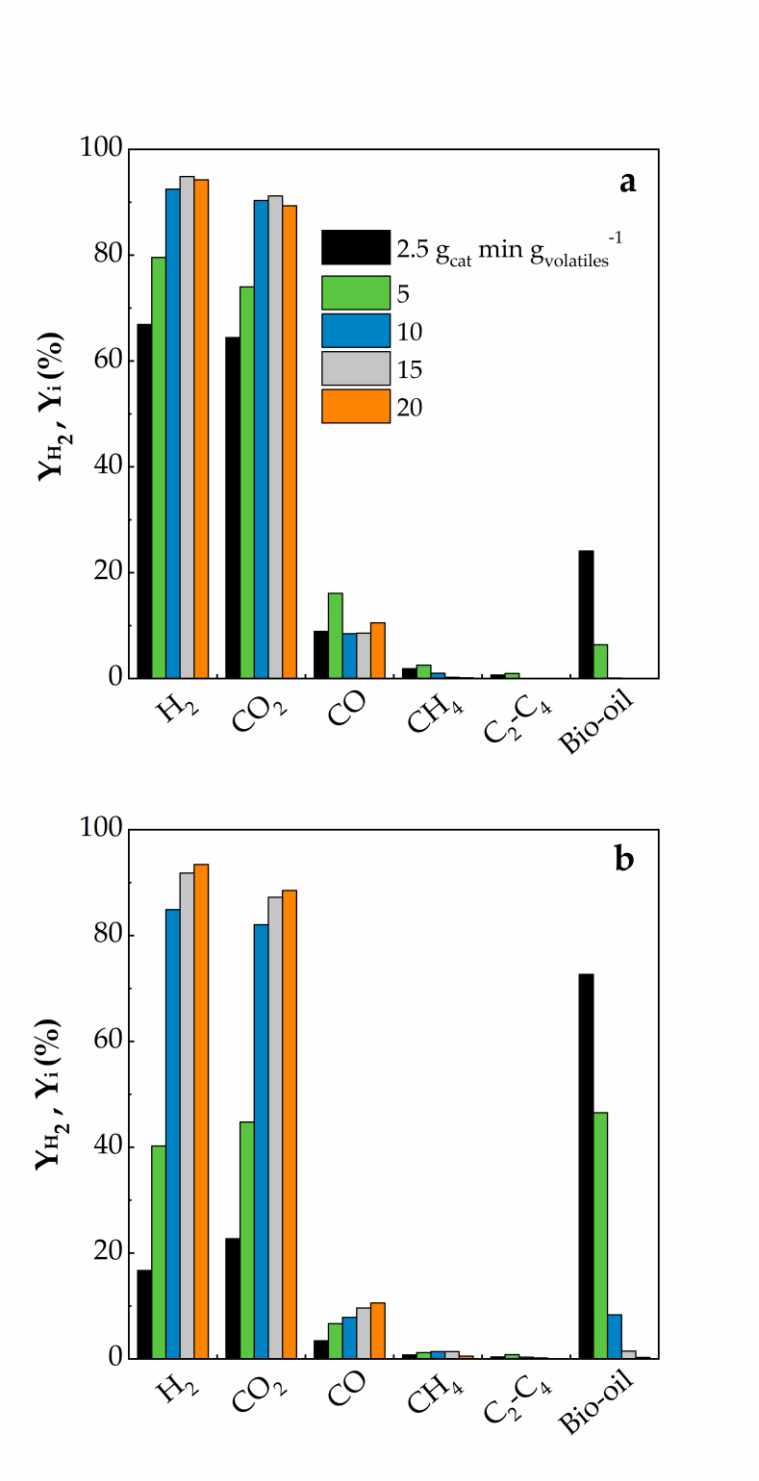

Figure 3. Individual product yields obtained with different space time values. a) Fixed bed and b) fluidized bed.

3.3. Catalyst stability

Fast catalyst deactivation rate is one of the most relevant challenges faced by the reforming of both bio-oil and biomass pyrolysis volatiles (Arregi et al., 2018a; Trane et al., 2012). Accordingly, the comparison of the deactivation processes operating with fluidized bed and fixed bed reactors is essential. The evolution of the reforming conversion with time on stream using both reactors is shown in Figure 4. As observed, operation under fixed bed regime led to higher conversion values and lower deactivation rates for all the studied space times. As explained in the previous section, the fluidized bed provides a poorer contact between the catalyst and the volatile stream due to mainly gas by-passing in the form of bubbles, which leads to lower conversion values. Moreover, the deactivation behavior is strongly conditioned by the composition of the reaction environment. In fact, catalyst deactivation in this process is mainly due to coke deposition, with the biomass derived oxygenates being the main coke precursors (Arregi et al., 2018b; Trane-Restrup and Jensen, 2015; Chen, Sun and Wang, 2017b; Santamaria et al., 2019b). A fluidized bed reactor ensures a well-mixed regime for the catalyst, with all catalyst particles having a similar contact with pyrolysis volatiles, and therefore a similar deactivation level at a given time. However, the situation in the fixed bed is completely different. In fact, the catalyst located at the initial section of the bed inlet undergoes fast deactivation, as the particles in this stretch are the first to be in contact with the product from the pyrolysis step. The deactivation front is initially close to the inlet, but gradually moves towards the outlet as time on stream is longer, until the entire bed of catalyst is deactivated.

This effect is clearly observed in the evolution of conversion with time on stream shown in Figure 4 for fixed and fluidized beds. Thus, the former allows attaining full conversion until a given time corresponding to the arrival of the deactivation front to the end of the catalyst bed. Subsequent to this time, conversion decreases in a sharp way. In

the fluidized bed however, reforming conversion decreases steadily until the catalyst has undergone severe deactivation, and in a pronounced way when the whole bed is considerably deactivated. Moreover, the deactivation in the reforming of biomass pyrolysis volatiles is of autocatalytic nature (Arregi et al., 2018b). Thus, the higher concentration of oxygenates in the reaction environment, as well as the partial deactivation of the catalyst, accelerate coke deposition, and consequently the deactivation process. The lower conversion in the fluidized bed reactor leads to a more pronounced deactivation. Moreover, the effect of H_2 in the attenuation of coke formation should also be considered (Bartholomew, 2001). Consequently, the lower H_2 partial pressure in the fluidized bed reactor contributes to enhancing deactivation in this reactor. This difference in the behavior of fluidized and fixed bed reactors was also observed under conditions in which conversion is full at the reactor outlet. Thus, operating with a space time of 20 g_{cat} min g_{vol}^{-1}, a conversion higher than 95 % was attained for 85 min on stream using a fluidized bed, whereas this conversion was maintained for longer than 100 min in the fixed bed (Figure 4). Similarly, a better performance of the fixed bed reactor was also evidenced for lower space times

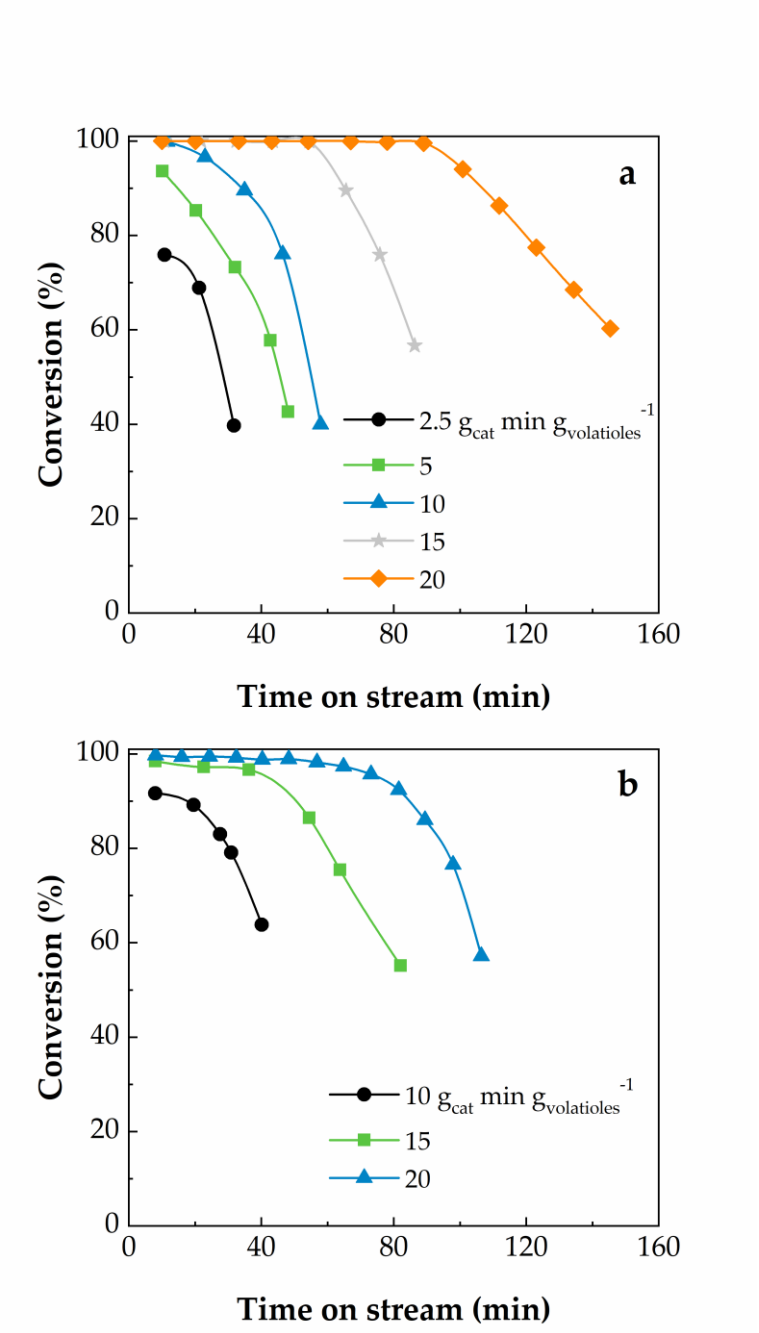

Figure 4. Evolution of the reforming conversion with time on stream for different space time values. a) Fixed bed and b) fluidized bed.

Figure 5 shows the evolution of product yields with time on stream obtained in the fixed and fluidized bed reforming reactors with space times of 10 and 20 g_{cat} min g_{vol}^{-1}. It should be noted that the time scales of the fixed bed are different to those of the fluidized bed. As observed, long times on stream led to a reduction in H_2 and CO_2

yields, which is associated with the deactivation of the catalyst for WGS (Eq. (7)) and reforming (Eqs (6) and (9)) reactions. However, there is no clear trend in the evolution of CO yield, as its lower formation rate in the reforming reaction due to deactivation was compensated by its lower conversion to CO_2 by WGS reaction. Furthermore, the yield of oxygenated compounds in the bio-oil increases with time on stream due to the lower extent of the reforming reaction. Finally, the yields of CH_4 and other light hydrocarbons are low, even when catalysts deactivation is remarkable, as these compounds are formed by secondary cracking reactions competing with reforming ones (Fu et al., 2014b; Bimbela et al., 2013). However, the relative low temperature and limited residence time in the reforming reactor attenuated cracking reactions and the formation of these compounds.

The analysis of the evolution of product yields also revealed the better performance of fixed bed reactor in the attenuation of catalyst deactivation. Thus, operating with a space time of 20 g_{cat} min $g_{volatiles}^{-1}$, hydrogen yield was maintained above 90 % for more than 90 min continuous operation in the fixed bed, whereas the yield dropped below this value subsequent to 65 min operation in the fluidized bed. Moreover, the shape of hydrogen (and CO_2) yield curves, with acceleration in their decreasing rate, clearly reveals the aforementioned autocatalytic effect, with this trend being more pronounced in the case of the fluidized bed reactor.

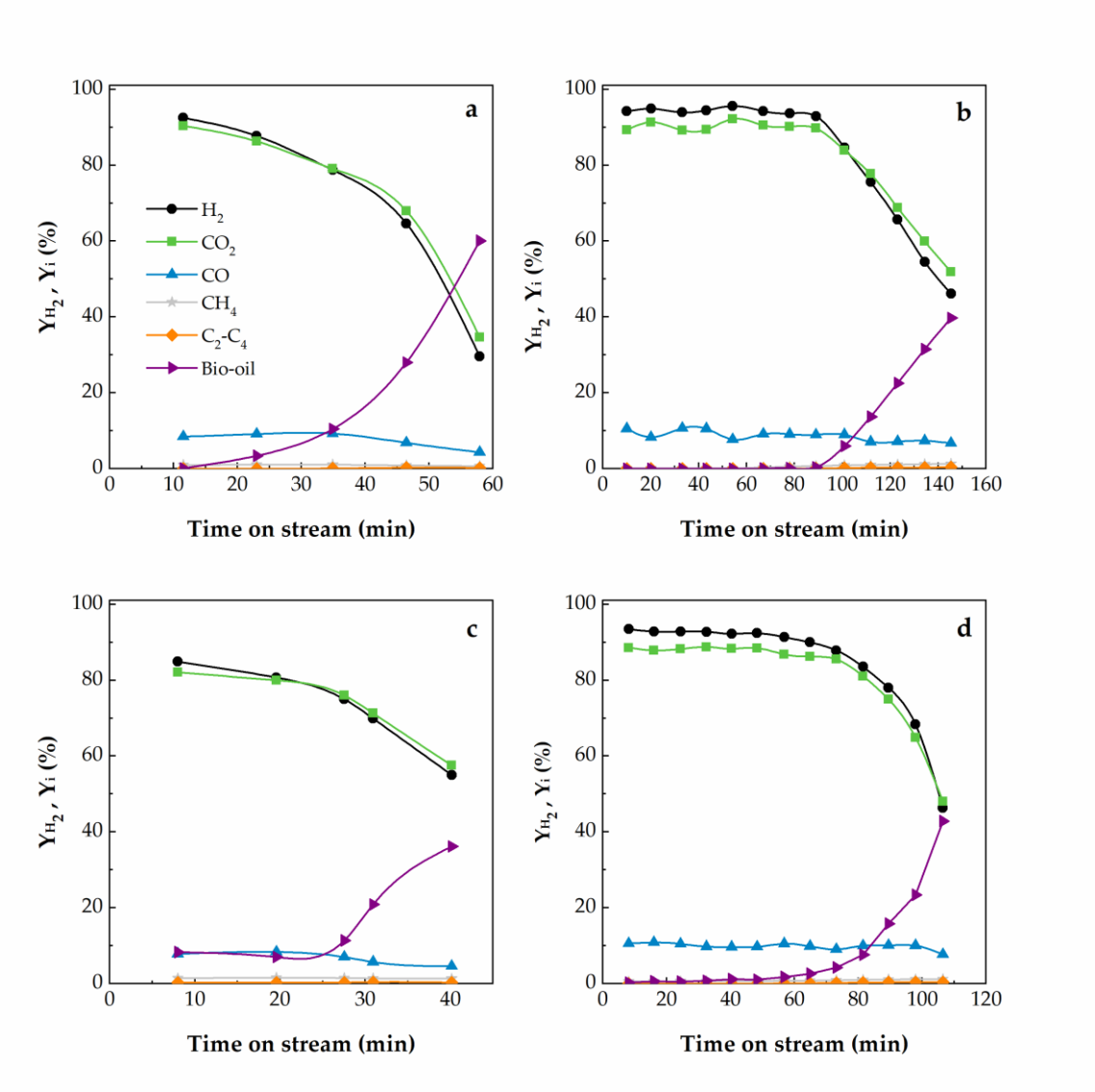

Figure 5. Evolution of product yields with time on stream for different space time values. a) Fixed bed, 10 g_{cat} min $g_{volatiles}^{-1}$, b) Fixed bed, 20 g_{cat} min $g_{volatiles}^{-1}$, c) Fluidized bed, 10 g_{cat} min $g_{volatiles}^{-1}$ and d) Fluidized bed 20 g_{cat} min $g_{volatiles}^{-1}$.

3.4. Coke deposition

The steam reforming of oxygenates is affected by fast catalyst deactivation, with coke formation and metal sintering being the main causes (Bartholomew, 2001; Argyle and Bartholomew, 2015). Metal sintering is a physical process of metal crystallite migration and coalescence, which is controlled by mainly temperature. This process causes a

reduction in the available active metal surface, and therefore a loss of catalytic activity (Argyle and Bartholomew, 2015). However, the low reforming temperature used in this study, i.e., only slightly higher than Ni Tamman temperature (590 ºC), avoids major Ni sintering, as reported in a previous detailed analysis of the deactivation involving these catalysts (Ochoa et al., 2018). Accordingly, the main cause of catalyst deactivation in this process is coke deposition. This section deals with the influence the reforming reactor design has on coke deposition and nature. It is to note that the catalysts analyzed in this section have been used for different times on stream due to their different deactivation rates in the runs with different space times in different reactor designs. Temperature programmed oxidation (TPO) was used for determining coke content in the catalyst samples (see section 2.2.)

Figure 6 shows the average coke deposition per biomass mass unit fed into the reactor for different space times. It should be noted that the duration of the runs and the amount of biomass fed depends on the deactivation rate, as all the runs were stopped when a similar final conversion value was reached (50-60%). As observed, operation in the fluidized bed reactor caused a higher coke deposition in relation to that obtained in the fixed bed. These results are consistent with the evolution of conversion with time on stream observed for the fixed and fluidized bed reactors (see Figure 4); that is, coke deposition rate is higher in the fluidized bed due to higher deactivation rate. Lan et al. (Lan et al., 2010) observed higher coke deposition rates in the steam reforming of bio-oil in the fixed bed reactor than in the fluidized bed. Nevertheless, this result may be conditioned by the higher S/C ratios they used in the fluidized bed operation. In fact, an increase in steam partial pressure not only promotes in situ coke gasification, but also reduces reactant partial pressure, and therefore coking reactions, with the subsequent

reduction of coke content (Garcia et al., 2000; Wang et al., 2007; Li et al., 2009; Arregi et al., 2018b; Fu et al., 2014a).

Moreover, Figure 6 also shows that an increase in space time caused a remarkable reduction in the coke deposition rate. This fact is related to the higher conversion obtained with high space times, which reduces the concentration of coke promoters, especially phenols and aldehydes, and minimizes their deposition. A similar effect of space time on coke deposition has been reported in the literature on the steam reforming of bio-oil and biomass fast pyrolysis volatiles (Valle et al., 2018; Arregi et al., 2018b).

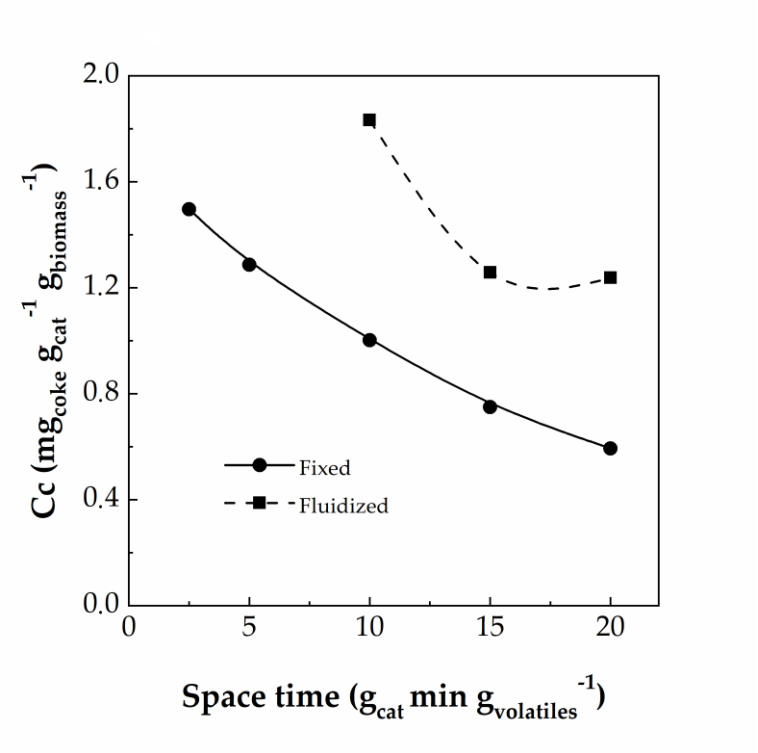

Figure 6. Coke deposited per biomass mass unit fed in the runs for different space times in fixed and fluidized reforming reactors.

A detailed analysis of the TPO curves provides information on the nature and location of the coke deposited in the spent catalysts, and therefore contributes to understanding the deactivation mechanism. Figures 7a and 7b show the TPO curves of the cokes obtained at different space time values in fixed and fluidized bed reactors, respectively. These curves clearly reveal the presence of two main coke species, whose

characteristics have been described in the literature on the reforming of oxygenates (Arregi et al., 2018b; Valle et al., 2018; Bimbela et al., 2012; Nogueira et al., 2014), and are as follows: i) Coke I: This coke is located close to Ni metallic sites, which not only promote its combustion at low temperatures (<450 ºC), but also its in situ gasification throughout the reforming process. This coke encapsulates Ni sites and is mainly of amorphous nature. ii) Coke II: This coke is located in the support, but not covering the Ni sites. Accordingly, its combustion is not activated by the metal and takes place at higher temperatures (450 to 600 ºC). This coke is more condensed and structured as time on stream is longer. The main precursors of this coke are CO, CH_4 and hydrocarbons, which are formed by means of Boudouard and decomposition reactions. Moreover, a minor peak is observed at even higher temperatures (> 650 ºC), which is due to the decomposition of the $CaCO_3$ formed by carbonation of the CaO included in the catalyst formulation.

In spite of the similar nature of the cokes deposited on the catalysts in fixed and fluidized bed reactors, differences are observed concerning their amounts. Thus, a higher amount of Coke II is observed in the samples taken from the fluidized bed reactor. This result is evidence that the formation of the two types of coke occurs sequentially, i.e., once the metal sites have been blocked by coke I, the higher concentration of oxygenates in the reaction environment in the fluidized reactor leads to the subsequent formation of coke II.

As space time was increased, the peaks shifted to higher temperatures for the catalysts used in both the fixed bed and the fluidized bed. This fact is due to the increase in time on stream, which favored the evolution of coke towards more ordered and stable structures, whose combustion temperatures are higher (Arregi et al., 2018b). Moreover,

although the coke is preferably deposited close to the metallic sites for short times on stream, it becomes more condensed and structured as the reaction evolves, and deposits are located at further positions from the sites on the catalyst surface, and therefore lead to the mentioned displacement of the peaks in the TPO profile.

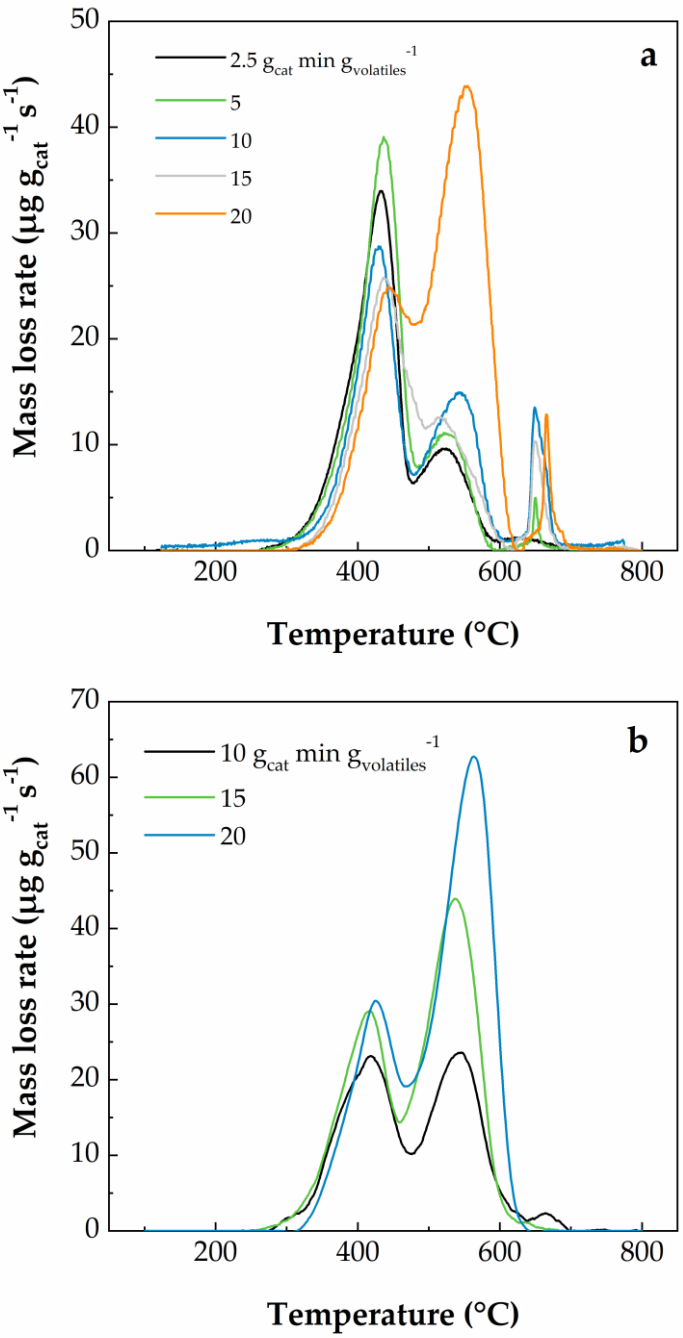

Figure 7. TPO profiles of the deactivated catalysts obtained if fixed (7a) and fluidized (7b).

4. Discussion

As stated in the previous sections, the fixed bed reactor showed a higher capacity for the in-line transformation of biomass pyrolysis volatiles into a hydrogen rich syngas. Thus, for the different space times analyzed, the fixed bed reactor was able to reach higher conversion values. In addition, it also showed a lower coke deposition, and consequently a lower deactivation rate. However, these differences were minimized as the space time of the catalyst was higher (see Figure 2). Thus, when the results obtained at 20 g_{cat} min g_{vol}^{-1} are analyzed, the initial conversion and the hydrogen yield and production are almost identical. Comparing the catalyst activity decay over the reforming reaction time, Figure 4, the highest space time studied is able to keep full conversion for almost 90 min on stream in the fixed bed reactor, whereas a conversion of 99 % may only be maintained for 50 min in the fluidized bed. Nevertheless, there is low deactivation rate at the beginning of the reaction in the fluidized bed, and high conversions (> 95 %) are therefore obtained in the first 75 min. Conversion drastically falls when either catalyst deactivation is significant in the fluidized bed or the deactivation front has reached the outlet of the reactor in the fixed bed. The complex composition of the biomass pyrolysis volatiles leads to rapid deactivation in both configurations, making necessary to regenerate or replace the catalyst every few minutes. Accordingly, the development of regeneration strategies plays a key role in the selection of the full-scale reactor design for operating in the pyrolysis-reforming process.

Therefore, given that differences in conversion and deactivation between the fixed and fluidized bed reactors are attenuated at high space time values, additional factors should be considered for the selection of the reforming reactor. Thus, fluidized beds have certain practical advantages over fixed beds from a scale up perspective. Accordingly, the intrinsic characteristics of biomass pyrolysis volatiles should be carefully

considered. Thus, steam reforming is a highly endothermic process, and high heat flow rates are therefore required to ensure operation under isothermal conditions (Arregi et al., 2018a; Guan et al., 2016; Ayalur Chattanathan, Adhikari and Abdoulmoumine, 2012; Chen, Sun and Wang, 2017b). In this respect, the fluidized bed reactor allows transferring higher heat rates and controlling better operating conditions due to the solid phase mixing regime. In fact, full-scale fixed beds hinder a good control of process temperature due to the uneven distribution of the reaction zone (and therefore heat demand) and radial heat transfer limitations. In these reactors, scaling up requires configurations based on parallel-bed small diameter multitubular reactors. This arrangement has a more complex design and higher capital and operating costs than the fluidized reactor.

In the same line, oxidative steam reforming by injecting oxygen in the reforming reactor has been proposed to face process endothermicity (Nahar and Dupont, 2013; Cai et al., 2008). This strategy can also contribute to attenuating catalysts deactivation rate, given that coke combustion is also promoted. In this case, the solid circulation regime and excellent gas-solid contact in fluidized beds may avoid the formation of hot spots, high oxygen partial pressure regions in the reactor and temperature control issues. This point is critical to ensure catalyst stability and prevent sintering or oxidation of the catalyst metallic phase.

Moreover, the development of the pyrolysis and in-line reforming process is greatly conditioned by the fast deactivation rate of the catalysts (Arregi et al., 2018a; Pandey, Prajapati and Sheth, 2019; Lopez et al., 2018). Although the fixed bed showed in this respect a slightly better performance, especially when operating with low space times, the deactivation rate was rather high (differences are less significant when operating with high space times). This fact makes necessary the development of advanced

regeneration strategies for the full-scale operation. Once again, fluidized bed reactors provide greater versatility, as catalyst circulation strategies between reaction and regeneration units can be implemented. It should be also taken into account that severe coke deposition may occur under certain conditions, as when operating with low steam/biomass ratios (Arregi et al., 2018b; Barbarias et al., 2018a; Valle et al., 2018) or handling feedstocks with high coke formation tendency, such as waste plastics (Erkiaga et al., 2015). This severe coke formation causes major operational problems in the fixed bed regime, such as bed plugging (Erkiaga et al., 2015; Medrano et al., 2011; Zhang et al., 2011; Li et al., 2009).

Obviously, certain essential aspects should be considered pertaining fluidized bed reactors, such as higher design complexity and investment or the problems associated with catalysts attrition. However, the features involving the reforming of pyrolysis volatiles, such as energy requirements and fast reactivation rates, make the fluidized bed a suitable alternative for full-scale operation.

5. Conclusions

The combination of biomass fast pyrolysis in a conical spouted bed and the in-line reforming of the volatiles in fixed or fluidized bed reactors has proven a great capacity for hydrogen production. Thus, hydrogen production reached 11 wt.% in both reactor designs under suitable conditions. It is to note that the fixed bed reactor showed a higher efficiency for the conversion of pyrolysis volatiles to hydrogen rich syngas. This fact is related to gas by-passing in fluidized beds, which reduces reactant conversion.

Furthermore, coke deposition rate was lower in the fixed bed than in the fluidized bed due mainly to the lower concentration of oxygenates in the reaction environment, as these compounds have a key role as coke precursors.

However, the differences in the performance of the two reactor configurations vanish at high space time values, for which full conversion was attained. Therefore, the selection of the reforming reactor for full-scale operation should be carefully addressed considering specifically the challenges associated with steam reforming, as are fast deactivation and endothermicity. In this sense, the fluidized bed reactor has several practical advantages for full-scale operation, as it ensures a better control of process conditions and allows for implementing advanced catalyst regeneration strategies and operation under oxidative reforming conditions.

Acknowledgments

This work was carried out with the financial support from Spain's ministries of Economy and Competitiveness (CTQ2016-75535-R (AEI/FEDER, UE) and Science, Innovation and Universities (RTI2018-101678-B-I00 (MCIU/AEI/FEDER, UE)), the European Union's Horizon 2020 research and innovation programme under the Marie Skłodowska-Curie grant agreement No. 823745, and the Basque Government (IT1218-19 and KK-2020/00107).

References

Adnan, M.A., Adamu, S., Muraza, O., Hossain, M.M., 2018. Fluidizable NiO–Fe2O3/SiO2–γAl2O3 for tar (toluene) conversion in biomass gasification, Process Saf. Environ. Prot. 116, 754-762.

Alvarez, J., Amutio, M., Lopez, G., Santamaria, L., Bilbao, J., Olazar, M., 2019. Improving bio-oil properties through the fast co-pyrolysis of lignocellulosic biomass and waste tyres, Waste Manage. 85, 385-395.

Alvarez, J., Kumagai, S., Wu, C., Yoshioka, T., Bilbao, J., Olazar, M., 2014. Hydrogen production from biomass and plastic mixtures by pyrolysis-gasification, 39, 10883-10891.

Alvarez, J., Lopez, G., Amutio, M., Mkhize, N.M., Danon, B., van der Gryp, P., Görgens, J.F., Bilbao, J., Olazar, M., 2017. Evaluation of the properties of tyre pyrolysis oils obtained in a conical spouted bed reactor, Energy. 128, 463-474.

Alvarez, J., Hooshdaran, B., Cortazar, M., Amutio, M., Lopez, G., Freire, F.B., Haghshenasfard, M., Hosseini, S.H., Olazar, M., 2018. Valorization of citrus wastes by fast pyrolysis in a conical spouted bed reactor, Fuel. 224, 111-120.

Amutio, M., Lopez, G., Artetxe, M., Elordi, G., Olazar, M., Bilbao, J., 2012. Influence of temperature on biomass pyrolysis in a conical spouted bed reactor, Resour. Conserv. Recycl. 59, 23-31.

Argyle, M.D., Bartholomew, C.H., 2015. Heterogeneous catalyst deactivation and regeneration: A review, Catalysts 5, 145-269.

Arregi, A., Lopez, G., Amutio, M., Barbarias, I., Bilbao, J., Olazar, M., 2016. Hydrogen production from biomass by continuous fast pyrolysis and in-line steam reforming, RSC Adv. 6, 25975-25985.

Arregi, A., Amutio, M., Lopez, G., Artetxe, M., Alvarez, J., Bilbao, J., Olazar, M., 2017. Hydrogen-rich gas production by continuous pyrolysis and in-line catalytic reforming of pine wood waste and HDPE mixtures, Energy Convers. Manage. 136, 192-201.

Arregi, A., Amutio, M., Lopez, G., Bilbao, J., Olazar, M., 2018a. Evaluation of thermochemical routes for hydrogen production from biomass: A review, Energy Convers. Manage. 165, 696-719.

Arregi, A., Lopez, G., Amutio, M., Artetxe, M., Barbarias, I., Bilbao, J., Olazar, M., 2018b. Role of operating conditions in the catalyst deactivation in the in-line steam reforming of volatiles from biomass fast pyrolysis, Fuel. 216, 233-244.

Artetxe, M., Lopez, G., Amutio, M., Barbarias, I., Arregi, A., Aguado, R., Bilbao, J., Olazar, M., 2015. Styrene recovery from polystyrene by flash pyrolysis in a conical spouted bed reactor, Waste Manage. 46, 126-133.

Ayalur Chattanathan, S., Adhikari, S., Abdoulmoumine, N., 2012. A review on current status of hydrogen production from bio-oil, Renewable Sustainable Energy Rev. 16, 2366-2372.

Balat, H., Kirtay, E., 2010. Hydrogen from biomass - Present scenario and future prospects, Int. J. Hydrogen Energy 35, 7416-7426.

Barbarias, I., Artetxe, M., Lopez, G., Arregi, A., Bilbao, J., Olazar, M., 2018a. Influence of the conditions for reforming HDPE pyrolysis volatiles on the catalyst deactivation by coke, Fuel Process. Technol. 171, 100-109.

Barbarias, I., Lopez, G., Alvarez, J., Artetxe, M., Arregi, A., Bilbao, J., Olazar, M., 2016. A sequential process for hydrogen production based on continuous HDPE fast pyrolysis and in-line steam reforming, Chem. Eng. J. 296, 191-198.

Barbarias, I., Lopez, G., Artetxe, M., Arregi, A., Bilbao, J., Olazar, M., 2018b. Valorisation of different waste plastics by pyrolysis and in-line catalytic steam reforming for hydrogen production, Energy Convers. Manage. 156, 575-584.

Bartholomew, C.H., 2001. Mechanisms of catalyst deactivation, Appl. Catal. A Gen. 212, 17-60.

Basagiannis, A.C., Verykios, X.E., 2007. Steam reforming of the aqueous fraction of bio-oil over structured Ru/MgO/Al2O3 catalysts, Catal. Today 127, 256-264.

Bimbela, F., Chen, D., Ruiz, J., García, L., Arauzo, J., 2012. Ni/Al coprecipitated catalysts modified with magnesium and copper for the catalytic steam reforming of model compounds from biomass pyrolysis liquids, Appl. Catal. B Environ. 119-120, 1-12.

Bimbela, F., Oliva, M., Ruiz, J., García, L., Arauzo, J., 2013. Hydrogen production via catalytic steam reforming of the aqueous fraction of bio-oil using nickel-based coprecipitated catalysts, Int. J. Hydrogen Energy 38, 14476-14487.

Bunma, T., Kuchonthara, P., 2018. Synergistic study between CaO and MgO sorbents for hydrogen rich gas production from the pyrolysis-gasification of sugarcane leaves, Process. Saf. Environ. Prot. 118, 188-194.

Cai, W., Wang, F., Zhan, E., Van Veen, A.C., Mirodatos, C., Shen, W., 2008. Hydrogen production from ethanol over Ir/CeO2 catalysts: A comparative study of steam reforming, partial oxidation and oxidative steam reforming, J. Catal. 257, 96-107.

Cao, J., Shi, P., Zhao, X., Wei, X., Takarada, T., 2014. Catalytic reforming of volatiles and nitrogen compounds from sewage sludge pyrolysis to clean hydrogen and synthetic gas over a nickel catalyst, Fuel Process. Technol. 123, 34-40.

Chai, Y., Gao, N., Wang, M., Wu, C., 2020. H2 production from co-pyrolysis/gasification of waste plastics and biomass under novel catalyst Ni-CaO-C, Chem. Eng. J. 382, 122947.

Chen, F., Wu, C., Dong, L., Vassallo, A., Williams, P.T., Huang, J., 2016. Characteristics and catalytic properties of Ni/CaAlOx catalyst for hydrogen-enriched syngas production from pyrolysis-steam reforming of biomass sawdust, Appl. Catal. B Environ. 183, 168-175.

Chen, J., Sun, J., Wang, Y., 2017. Catalysts for Steam Reforming of Bio-oil: A Review, Ind. Eng. Chem. Res. 56, 4627-4637.

Claude, V., Courson, C., Köhler, M., Lambert, S.D., 2016. Overview and Essentials of Biomass Gasification Technologies and Their Catalytic Cleaning Methods, Energy Fuels. 30, 8791-8814.

Dong, L., Wu, C., Ling, H., Shi, J., Williams, P.T., Huang, J., 2017. Promoting hydrogen production and minimizing catalyst deactivation from the pyrolysis-catalytic steam reforming of biomass on nanosized NiZnAlOx catalysts, Fuel 188, 610-620.

Efika, C.E., Wu, C., Williams, P.T., 2012. Syngas production from pyrolysis-catalytic steam reforming of waste biomass in a continuous screw kiln reactor, J. Anal. Appl. Pyrolysis 95, 87-94.

Erkiaga, A., Lopez, G., Barbarias, I., Artetxe, M., Amutio, M., Bilbao, J., Olazar, M., 2015. HDPE pyrolysis-steam reforming in a tandem spouted bed-fixed bed reactor for H2 production, J. Anal. Appl. Pyrolysis.116, 34-41.

Font Palma, C., 2013. Modelling of tar formation and evolution for biomass gasification: A review, Appl. Energy 111, 129-141.

Fu, P., Yi, W., Li, Z., Bai, X., Zhang, A., Li, Y., Li, Z., 2014. Investigation on hydrogen production by catalytic steam reforming of maize stalk fast pyrolysis bio-oil, Int. J. Hydrogen Energy 39, 13962.

Gai, C., Zhu, N., Hoekman, S.K., Liu, Z., Jiao, W., Peng, N., 2019. Highly dispersed nickel nanoparticles supported on hydrochar for hydrogen-rich syngas production from catalytic reforming of biomass, Energy Convers. Manage. 183, 474-484.

Gao, N., Liu, S., Han, Y., Xing, C., Li, A., 2015. Steam reforming of biomass tar for hydrogen production over NiO/ceramic foam catalyst, 40, 7983-7990.

Garcia, L., French, R., Czernik, S., Chornet, E., 2000. Catalytic steam reforming of bio-oils for the production of hydrogen: effects of catalyst composition, Appl. Catal. A. Gen. 201, 225.

Garcia-Nunez, J.A., Pelaez-Samaniego, M.R., Garcia-Perez, M.E., Fonts, I., Abrego, J., Westerhof, R.J.M., Garcia-Perez, M., 2017. Historical Developments of Pyrolysis Reactors: A Review, Energy Fuels 31, 5751-5775.

Guan, G., Kaewpanha, M., Hao, X., Abudula, A., 2016. Catalytic steam reforming of biomass tar: Prospects and challenges, Renewable Sustainable Energy Rev. 58, 450-461.

Heidenreich, S., Foscolo, P.U., 2015. New concepts in biomass gasification, Prog. Energy Combust. Sci. 46, 72-95.

Kaewpanha, M., Karnjanakom, S., Guan, G., Hao, X., Yang, J., Abudula, A., 2017. Removal of biomass tar by steam reforming over calcined scallop shell supported Cu catalysts, J. Energy Chem. 26, 660-666.

Kumagai, S., Alvarez, J., Blanco, P.H., Wu, C., Yoshioka, T., Olazar, M., Williams, P.T., 2015. Novel Ni-Mg-Al-Ca catalyst for enhanced hydrogen production for the pyrolysis-gasification of a biomass/plastic mixture, J. Anal. Appl. Pyrolysis. 113, 15-21.

Kumagai, S., Yabuki, R., Kameda, T., Saito, Y., Yoshioka, T., 2019. Simultaneous recovery of H2-rich syngas and removal of HCN during pyrolytic recycling of polyurethane by Ni/Mg/Al catalysts, Chem. Eng. J. 361, 408-415.

Kunii, D., Levenspiel, O., 2013. Fluidization Engineering, 2º ed. Elsevier.

Lan, P., Xu, Q., Zhou, M., Lan, L., Zhang, S., Yan, Y., 2010. Catalytic steam reforming of fast pyrolysis bio-oil in fixed bed and fluidized bed reactors, Chem. Eng. Technol. 33, 2021.

Li, H., Xu, Q., Xue, H., Yan, Y., 2009. Catalytic reforming of the aqueous phase derived from fast-pyrolysis of biomass, Renew. Energy 34, 2872-2877.

Liu, S., Chen, M., Chu, L., Yang, Z., Zhu, C., Wang, J., Chen, M., 2013. Catalytic steam reforming of bio-oil aqueous fraction for hydrogen production over Ni-Mo supported on modified sepiolite catalysts, Int. J. Hydrogen Energy 38, 3948-3955.

Lopez, G., Artetxe, M., Amutio, M., Alvarez, J., Bilbao, J., Olazar, M., 2018. Recent advances in the gasification of waste plastics. A critical overview, Renewable Sustainable Energy Rev. 82, 576-596.

Lopez, G., Artetxe, M., Amutio, M., Bilbao, J., Olazar, M., 2017. Thermochemical routes for the valorization of waste polyolefinic plastics to produce fuels and chemicals. A review, Renewable Sustainable Energy Rev. 73, 346-368.

Medrano, J.A., Oliva, M., Ruiz, J., GarcÃa, L., Arauzo, J., 2011. Hydrogen from aqueous fraction of biomass pyrolysis liquids by catalytic steam reforming in fluidized bed, Energy 36, 2215.

Miyazawa, T., Kimura, T., Nishikawa, J., Kado, S., Kunimori, K., Tomishige, K., 2006. Catalytic performance of supported Ni catalysts in partial oxidation and steam reforming of tar derived from the pyrolysis of wood biomass, Catal Today 115, 254-262.

Moliner, C., Marchelli, F., Bosio, B., Arato, E., 2017. Modelling of spouted and spout-fluid beds: Key for their successful scale up, Energies 10, 1729.

Molino, A., Chianese, S., Musmarra, D., 2016. Biomass gasification technology: The state of the art overview, J. Energy Chem. 25, 10-25.

Moulijn, J., Van Diepen, A., Kapteijn, F., 2010. Activity loss, Handbook of Heterogeneous Catalysis. 1-17.

Nabgan, W., Tuan Abdullah, T.A., Mat, R., Nabgan, B., Gambo, Y., Ibrahim, M., Ahmad, A., Jalil, A.A., Triwahyono, S., Saeh, I., 2017. Renewable hydrogen production from bio-oil derivative via catalytic steam reforming: An overview, Renewable Sustainable Energy Rev. 79, 347-357.

Nahar, G., Dupont, V., 2013. Recent advances in hydrogen production via autothermal reforming process (ATR): A review of patents and research articles, Recent Pat. Chem. Eng. 6, 8-42.

Nogueira, F.G.E., Assaf, P.G.M., Carvalho, H.W.P., Assaf, E.M., 2014. Catalytic steam reforming of acetic acid as a model compound of bio-oil, Appl. Catal. B Environ. 160-161, 188-199.

Ochoa, A., Arregi, A., Amutio, M., Gayubo, A.G., Olazar, M., Bilbao, J., Castaño, P., 2018. Coking and sintering progress of a Ni supported catalyst in the steam reforming of biomass pyrolysis volatiles, Appl. Catal. B Environ. 233, 289-300.

Pandey, B., Prajapati, Y.K., Sheth, P.N., 2019. Recent progress in thermochemical techniques to produce hydrogen gas from biomass: A state of the art review Int. J. Hydrogen Energy 44, 25384-25415.

Park, Y., Namioka, T., Sakamoto, S., Min, T.j., Roh, S.a., Yoshikawa, K., 2010. Optimum operating conditions for a two-stage gasification process fueled by polypropylene by means of continuous reactor over ruthenium catalyst, Fuel Process Technol. 91, 951-957.

Parthasarathy, P., Narayanan, K.S., 2014. Hydrogen production from steam gasification of biomass: Influence of process parameters on hydrogen yield – A review, Renewable Energy 66, 570-579.

Perkins, G., Bhaskar, T., Konarova, M., 2018. Process development status of fast pyrolysis technologies for the manufacture of renewable transport fuels from biomass, Renewable Sustainable Energy Rev. 90, 292-315.

Remon, J., Medrano, J.A., Bimbela, F., Garcia, L., Arauzo, J., 2013. Ni/Al-Mg-O solids modified with Co or Cu for the catalytic steam reforming of bio-oil, Appl. Catal. B. Environ. 132-133, 433-444.

Remón, J., Broust, F., Valette, J., Chhiti, Y., Alava, I., Fernandez-Akarregi, A.R., Arauzo, J., Garcia, L., 2014. Production of a hydrogen-rich gas from fast pyrolysis bio-oils: Comparison between homogeneous and catalytic steam reforming routes, Int. J. Hydrogen Energy 39, 171-182.

Santamaria, L., Artetxe, M., Lopez, G., Cortazar, M., Amutio, M., Bilbao, J., Olazar, M., 2020. Effect of CeO2 and MgO promoters on the performance of a Ni/Al2O3 catalyst in the steam reforming of biomass pyrolysis volatiles, Fuel Process Technol. 198, 106223.

Santamaria, L., Lopez, G., Arregi, A., Amutio, M., Artetxe, M., Bilbao, J., Olazar, M., 2019a. Effect of calcination conditions on the performance of Ni/MgO-Al2O3 catalysts in the steam reforming of biomass fast pyrolysis volatiles, Catal. Sci. Technolog. 9, 3947-3963.

Santamaria, L., Lopez, G., Arregi, A., Amutio, M., Artetxe, M., Bilbao, J., Olazar, M., 2018. Influence of the support on Ni catalysts performance in the in-line steam reforming of biomass fast pyrolysis derived volatiles, Appl. Catal. B Environ. 229, 105-113.

Santamaria, L., Lopez, G., Arregi, A., Amutio, M., Artetxe, M., Bilbao, J., Olazar, M., 2019b. Stability of different Ni supported catalysts in the in-line steam reforming of biomass fast pyrolysis volatiles, Appl. Catal. B Environ. 242, 109-120.

Shahabuddin, M., Krishna, B.B., Bhaskar, T., Perkins, G., 2020. Advances in the thermo-chemical production of hydrogen from biomass and residual wastes: Summary of recent techno-economic analyses, Bioresour. Technol. 299, 122557.

Shen, Y., Areeprasert, C., Prabowo, B., Takahashi, F., Yoshikawa, K., 2014. Metal nickel nanoparticles in situ generated in rice husk char for catalytic reformation of tar and syngas from biomass pyrolytic gasification, RSC Adv. 4, 40651-40664.

Shen, Y., Yoshikawa, K., 2013. Recent progresses in catalytic tar elimination during biomass gasification or pyrolysis - A review, Renewable Sustainable Energy Rev. 21, 371-392.

Tanksale, A., Beltramini, J.N., Lu, G.M., 2010. A review of catalytic hydrogen production processes from biomass, Renewable Sustainable Energy Rev. 14, 166-182.

Trane, R., Dahl, S., Skjoth-Rasmussen, M.S., Jensen, A.D., 2012. Catalytic steam reforming of bio-oil, Int. J. Hydrogen Energy, 6447-6472.

Trane-Restrup, R., Jensen, A.D., 2015. Steam reforming of cyclic model compounds of bio-oil over Ni-based catalysts: Product distribution and carbon formation, Appl. Catal. B Environ. 165, 117-127.

Valderrama Rios, M.L., González, A.M., Lora, E.E.S., Almazán del Olmo, O.A., 2018. Reduction of tar generated during biomass gasification: A review, Biomass Bioenergy. 108, 345-370.

Valle, B., Aramburu, B., Benito, P.L., Bilbao, J., Gayubo, A.G., 2018. Biomass to hydrogen-rich gas via steam reforming of raw bio-oil over Ni/La2O3-AAl2O3 catalyst: Effect of space-time and steam-to-carbon ratio, Fuel 216, 445-455.

Wang, L., Li, D., Koike, M., Watanabe, H., Xu, Y., Nakagawa, Y., Tomishige, K., 2013. Catalytic performance and characterization of Ni-Co catalysts for the steam reforming of biomass tar to synthesis gas, Fuel 112, 654-661.

Wang, L., Li, D., Koike, M., Koso, S., Nakagawa, Y., Xu, Y., Tomishige, K., 2011. Catalytic performance and characterization of Ni-Fe catalysts for the steam reforming of tar from biomass pyrolysis to synthesis gas, Appl. Catal. A Gen. 392, 248-255.

Wang, Z., Pan, Y., Dong, T., Zhu, X., Kan, T., Yuan, L., Torimoto, Y., Sadakata, M., Li, Q., 2007. Production of hydrogen from catalytic steam reforming of bio-oil using C12A7-O--based catalysts, Appl. Catal. A General. 320, 24-34.

Wu, C., Williams, P.T., 2010. A novel Ni-Mg-Al-CaO catalyst with the dual functions of catalysis and CO2 sorption for H2 production from the pyrolysis-gasification of polypropylene, Fuel 89, 1435-1441.

Xiao, X., Cao, J., Meng, X., Le, D.D., Li, L., Ogawa, Y., Sato, K., Takarada, T., 2013. Synthesis gas production from catalytic gasification of waste biomass using nickel-loaded brown coal char, Fuel 103, 135-140.

Xiao, X., Meng, X., Le, D.D., Takarada, T., 2011. Two-stage steam gasification of waste biomass in fluidized bed at low temperature: Parametric investigations and performance optimization, Bioresour. Technol. 102, 1975-1981.

Yu, H., Liu, Y., Liu, J., Chen, D., 2019. High catalytic performance of an innovative Ni/magnesium slag catalyst for the syngas production and tar removal from biomass pyrolysis, Fuel 254, 115622.

Zhang, S., Li, X., Li, Q., Xu, Q., Yan, Y., 2011. Hydrogen production from the aqueous phase derived from fast pyrolysis of biomass, J. Anal. Appl. Pyrolysis. 92, 158-163.